

EFFECTS OF THREE-DIMENSIONAL FLOW INDUCED BY A UNILATERAL POLYP ON ENERGY TRANSFER AND VOCAL FOLD MOTION IN VOICED SPEECH

Byron D. Erath

Department of Mechanical and Aerospace Engineering
The George Washington University
205 Staughton Hall, 707 22nd St. NW, Washington, DC
erath@gwu.edu

Michael W. Plesniak

Department of Mechanical and Aerospace Engineering
The George Washington University
739 Phillips Hall, 801 22nd St. NW, Washington, DC
plesniak@gwu.edu

ABSTRACT

The evolution of three-dimensional glottal flow patterns arising from the presence of a unilateral polyp is presented. The polyp is modeled by a hemi-spheroid-like protuberance placed on the medial surface of 7.5 time scaled-up, driven vocal fold model. Particle image velocimetry measurements in both the streamwise and cross-stream directions identify the development of hairpin and horseshoe vortices during the closing phases of the phonatory cycle. These flow structures induce significant three-dimensional flow effects that are otherwise absent during normal vocal fold motion. Three-dimensional flow behavior is correlated to the energy exchange process that drives vocal fold motion.

INTRODUCTION

Voiced speech in humans results from a highly-complex process. When a critical lung pressure is achieved, the vocal folds are pushed apart by fluid loading, and the resultant coupling of the aerodynamic forces, tissue properties, and acoustic loadings incite self-sustained oscillations. These oscillations are characterized by a mucosal wave that propagates along the vocal fold surface, creating a temporally-varying orifice geometry, the glottis, that transitions from a convergent to divergent passage throughout the phonatory cycle (See Figure 1). During the closing phases, when the glottis forms a divergent passage, viscous flow phenomena

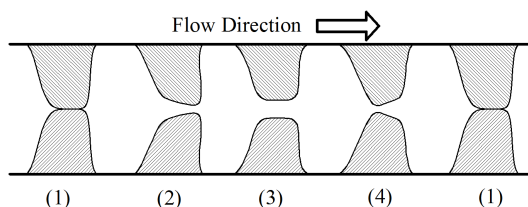


Figure 1: A representation of the phonatory cycle

dominate, shaping the pressure fields that drive vocal fold motion (Triep et al., 2005; Erath and Plesniak, 2006a; 2006b; Krane et al., 2007).

Pathologies can have devastating impacts on the ability to produce voiced speech, and thereby communicate. Although the ability to properly phonate is often taken for granted, the lifetime prevalence of voice disorders in the general population is almost 30%, and can reach as high as 60% in professional voice users, such as educators (Roy et al., 2004).

The most common voice disorders, which usually occur in the superficial layers of the lamina propria, are nodules and polyps. Developing as either unilateral or bilateral, these structural deformities begin as soft pliable tissue, but can become thicker and fibrosed over time. Usually developing due to abuse and/or overuse, they can develop from a single episode or chronic abuse (Titze, 1994). Common sessile polyps are geometric protuberances that resemble a hemi-spheroid-like protuberance on the medial vocal fold surface.

When polyps develop, vocal quality is degraded and a “weak” or “breathy” voice often results due to lack of complete glottal closure during the vocal fold cycle. In addition, aperiodic vibrations, temporal asymmetry and the onset of chaotic vocal fold motion has been observed in both *in-vivo* investigations of humans, and excised canine larynges (Baken, 1990; Berry et al., 1994; Zhang and Jiang, 2008).

Efforts to determine why unilateral polyps produce chaotic disordered vocal fold motion have focused exclusively on the perturbation of the vocal fold dynamics that results from an added mass on the vocal folds (Zhang and Jiang, 2004; 2008). In spite of the fundamental role that aerodynamic loading plays in generating vocal fold motion, disruption of these forces by a unilateral polyp has never been investigated.

The objective of this work is to experimentally investigate how the intraglottal flow field is disrupted by the presence of a unilateral polyp in a driven, scaled-up physical model of the human vocal folds

EXPERIMENTAL FACILITY AND METHODS

Laryngeal Flow Facility

Experimental flow investigations were performed in a pressure-driven flow facility that was designed explicitly for laryngeal flow investigations. Details of the facility can be found in Erath and Plesniak (2010a, 2010b). Compressed air (~100-120 psi) was regulated by a Nullmatic 40-100 pressure regulator to magnitudes representative of speech. Downstream of the regulator, the mean, time-averaged volumetric flow rate, Q_{mean} , was acquired as the air passed through a Dwyer Instruments rotameter. The air then passed through a TSI 6-jet Laskin nozzle olive oil atomizer, that created smoke particles ($O(1-5\mu\text{m})$) for flow diagnostics. The seeded flow enters the wind tunnel through a backward-facing perforated pipe before passing through honeycomb flow straighteners, followed by a 4:1 2D contraction ratio in the vertical (anterior-posterior) z direction, designed according to the cubic matching method of Morel (1977). The x direction aligns with the streamwise (inferior-superior) flow direction, and y is in the spanwise (medial-lateral) direction. The test section measures 9.14 cm high in the z direction, and 12.60 cm wide in the y direction. The flow quality of the test section was validated, with streamwise turbulence intensities less than 2%. The vocal folds are positioned in the wind tunnel with the leading edge 15.24 cm downstream of the start of the test section.

The vocal fold models were manufactured following the M5 specifications of Scherer et al. (2001), which extrude a constant 2D vocal fold geometry in the z direction. The models were scaled-up 7.5 time life-size. The medial surface of each model was rapid-prototyped from ABS plastic. Latex connected both the leading and trailing edges of each model to the walls of the wind tunnel, forming a closed geometry, and providing compliance. Figure 2 shows an image of the vocal folds placed in the wind tunnel, the orientation of the coordinate system, and the planes in which data were acquired.

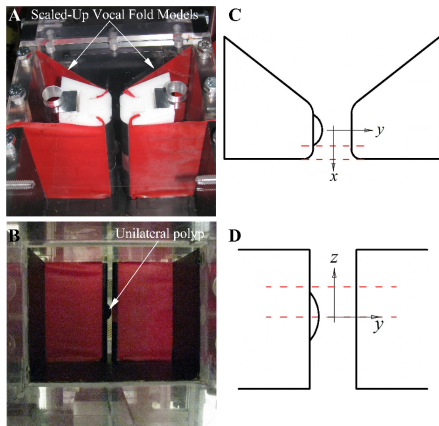


Figure 2: Images of the model vocal folds (left) and the orientation of the data planes (right).

The deformation of the medial vocal fold surface due to the presence of a unilateral polyp was produced by rapid-prototyping a unilateral polyp on one vocal fold wall. The scaled-up geometry was created by prescribing a circle of radius 0.889 cm on the medial surface and revolving it 180 degrees about a midline that was 0.340 cm from the edge of the radius. In this manner, an ellipsoidal protrusion is created with the major axis oriented in the z direction, measuring 1.397 cm long, 0.681 cm wide in the x direction, and protruding 0.340 cm from the surface in the y direction.

The mucosal wave of the vocal folds is reproduced in the models by independently driving each vocal fold with two stepper motors/drivers (Oriental Motors 400 oz-in/Velmex NF-90). For both vocal folds, one motor drives the linear medial-lateral displacement, while the other controls the angular rotation. Driven in tandem, the converging-diverging temporal variation of the glottal channel is reproduced. The vocal fold motion is prescribed with LabView v8.2 software, with an external trigger initiating the motion and synchronizing it with the data acquisition. Figure 3 shows the scaled-up motion of one vocal fold wall throughout a single phonatory cycle, where θ is the angular rotation of a vocal fold wall. Note that the polyp prevents complete glottal closure.

The fluid and motion parameters are presented in Table 1, where the scaled-up minimum glottal opening reaches a maximum, d , of 13.0 mm. The maximum glottal angle, Ψ , was prescribed at ± 30 degrees during vocal fold motion. The mean flow rate was $Q_{\text{mean}} = 1,373$ mL/s, which scales to a life-size flow rate of 183 mL/s. The Reynolds number based on the mean flow rate and d was 995. An oscillation period of $T = 0.600$ seconds scales to a life-size frequency of 93.8 Hz. The open quotient (OQ), defined as the time the vocal folds spend open (T_{open}) divided by the oscillation period (T), was 0.71, and the speed quotient, defined as the time for the vocal folds to go from closure to maximum opening divided by the time to go from maximum opening to closure, was 1.0.

Particle Image Velocimetry Measurements

Phase-averaged particle image velocimetry (PIV) data were acquired in order to quantify the inception of three-dimensional flow behavior arising from the presence of a unilateral polyp. Image pairs were acquired on a PowerView 4MP 2,000 x 2,000 pixel CCD camera. TSI Insight 3G software was used for timing, data acquisition, and vector

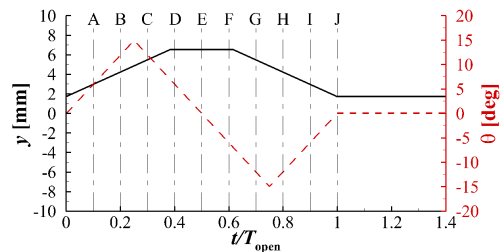


Figure 3: Linear and angular motion parameters used to drive vocal fold motion.

Table 1: Flow and motion parameters.

Parameter	Physiological	Driven Model (equivalent values)
Scale	1	7.5
d [mm]	1 - 3	13.0 (1.7)
Ψ [deg]	+/- 20 - 40	+/- 30
Q [mL/s]	~85 - 250	1,373 (183)
Re_{mean}	~300 - 2,000	995
f_0 [Hz]	~80 - 220	1.7 (93.8)
OQ	~0.5 - 0.9	0.71
SQ	~0.8 - 1.2	1.0

processing, with an external trigger synchronizing data acquisition with the vocal fold motion. Data were acquired in both the x - y and y - z planes, with the planes denoted by a dashed red line in Figure 2. In the x - y data plane (Figure 2D), flow in two planes was investigated at $z = 0$ cm (bisecting the polyp), and $z = 1$ cm. In the scaled-up x - y data plane, a total of $N_i = 300$ image pairs were acquired at 6 instances during the phonatory cycle, denoted in Figure 3 as points C – H, which correspond to times of $t/T_{\text{open}} = 0.3, 0.4, 0.5, 0.6, 0.7,$ and 0.8 , respectively. Image pairs were processed using a recursive Nyquist grid ($64 \times 64, 32 \times 32$, pixels). In the y - z data plane (Figure 2C), data were also acquired at two locations. The first was immediately downstream of the polyp at a scaled-up location of $x = 0.70$ cm, and the second was at the glottal exit corresponding to $x = 1.50$ cm. For both cases 300 image pairs were acquired at 10 phases, labeled in Figure 3 as A – I, corresponding to $t/T_{\text{open}} = 0.1 - 1.0$ at equally-spaced increments of 0.1. Data in the y - z plane were processed using a 64×64 pixel Nyquist grid. In both planes maximum and minimum velocity filters were applied.

RESULTS

The following section investigates the impact of a unilateral polyp on the glottal jet trajectory, as well as the inception of out-of-plane (normal to the streamwise direction) three-dimensional flow.

Glottal Jet Trajectory

The glottal jet trajectory was computed from the PIV images obtained in the x - y plane. The angular deflection of the glottal jet from the streamwise midline was found by computing a linear fit to the center of the jet, and computing the angular deflection, α , of the jet from the midline as proposed by Erath and Plesniak (2006a). Prior investigations have shown that for normal vocal fold motion, when the orientation of the jet trajectory is plotted as a percentage of instances (N/N_i), and as a function of normalized deflection angle ($2\alpha/\Psi$) a centrally-oriented distribution occurs during the opening phases, and then transitions to a bimodal distribution during the divergent phases, with approximately equal number of instances, N , attaching to each wall (Erath and Plesniak, 2006a; 2010a).

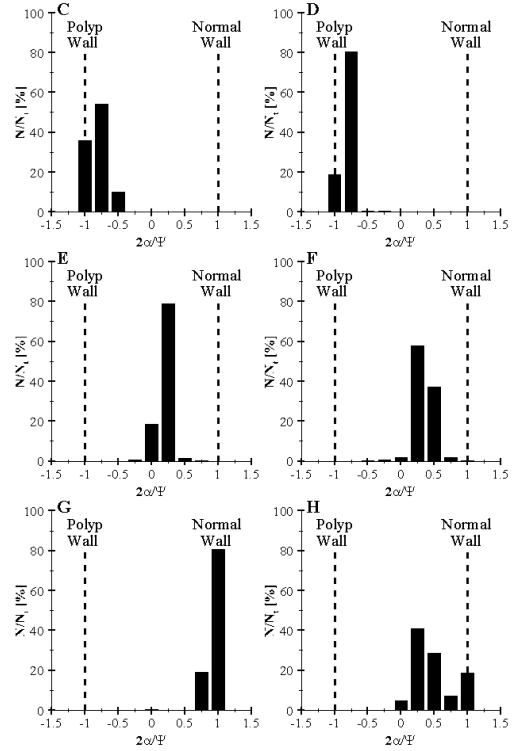


Figure 4: Histogram distribution of the jet trajectory in the x - y plane at $z = 0$ cm.

Figures 4 and 5 plot the jet trajectories as histogram distributions for flow in the x - y plane at $z = 0$ cm, and $z = 1$ cm, respectively. Figure 4 shows that during the opening phases the flow attaches to the (left) diseased wall, and then as the cycle progresses, separates from, and attaches to the wall opposite of the polyp. The flow trajectory appears relatively stable until the final phase, H ($t/T_{\text{open}} = 0.80$), where there is significant variation, although at no point during the cycle does the trajectory assume a bimodal distribution. At $z = 1$ cm (Figure 5) the flow remains centrally-oriented for all instances, except for at point G ($t/T_{\text{open}} = 0.70$) when a weak bimodal distribution is observed. The significant variation in the trajectory as a function of anterior-posterior location in the z direction suggests that the presence of the polyp significantly impacts what is considered “normal” flow behavior, i.e. no anterior-posterior gradients.

Figures 6 and 7 show the mean phase-averaged velocity fields, corresponding to Figures 4 and 5, respectively. The mean fields were computed by averaging only the image pairs whose jet trajectory was the same as the most dominant trajectory at the corresponding phase. Figure 6 confirms that the polyp induces downstream flow separation, and the jet moves from the diseased to the healthy wall during the later stages of the cycle. On the diseased wall, a stagnant region of flow recirculation is observed immediately downstream of the polyp. Vortex shedding from the polyp further impacts the flow behavior by causing a thinning of the jet width, and deflecting the downstream jet as it exits the glottis. This

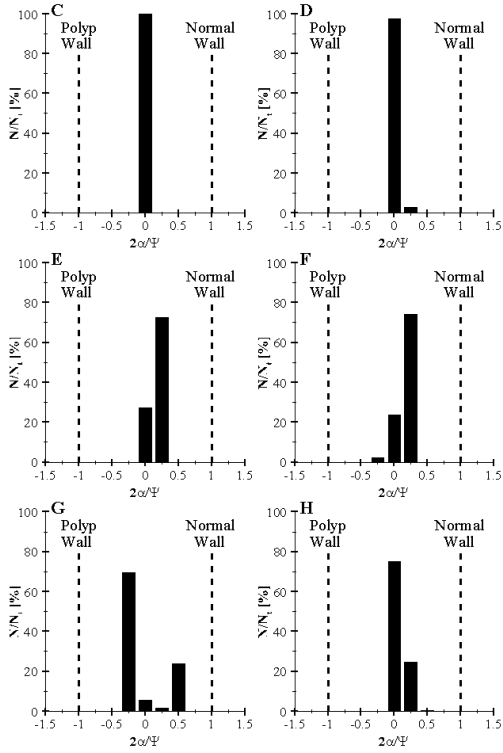


Figure 5: Histogram distribution of the jet trajectory in the x - y plane at $z = 1$ cm.

behavior is consistent with the formation of hairpin vortices as the flow is shed from the top of the polyp (Acarlar and Smith, 1987). Furthermore, it is of significance that the highest velocity magnitudes appear at a location downstream of the polyp, as opposed to at the minimal constriction.

Figure 7 shows the mean, phase-averaged velocity fields at 1 cm above the polyp. The trajectory remains centrally oriented-throughout the channel for the bulk of the cycle, with only slight excursions from the centerline observed. In comparing similar phases at the varying z locations in Figures 6 and 7, it becomes evident that flow attachment points along the medial vocal fold surface vary significantly.

Out-of-Plane Velocity Fields

The out-of-plane velocity fields (normal to the streamwise direction) are presented in Figures 8 and 9, at x locations of 0.7 and 1.5 cm, respectively. Note that the velocity scales differ between the figures. Data are presented at 10 instances during the phonatory cycle (see Figure 3), with the dashed lines indicating the position of the bounding walls. In Figure 9 the walls are spaced wider apart due to the expanding area caused by the exit radius.

During the opening phases of Figure 8 (Points A – C) the flow converges towards the midline, and towards the diseased wall. This can be explained by noting that the favorable pressure gradient associated with the convergent channel will inhibit separation, and the flow will largely follow the contour

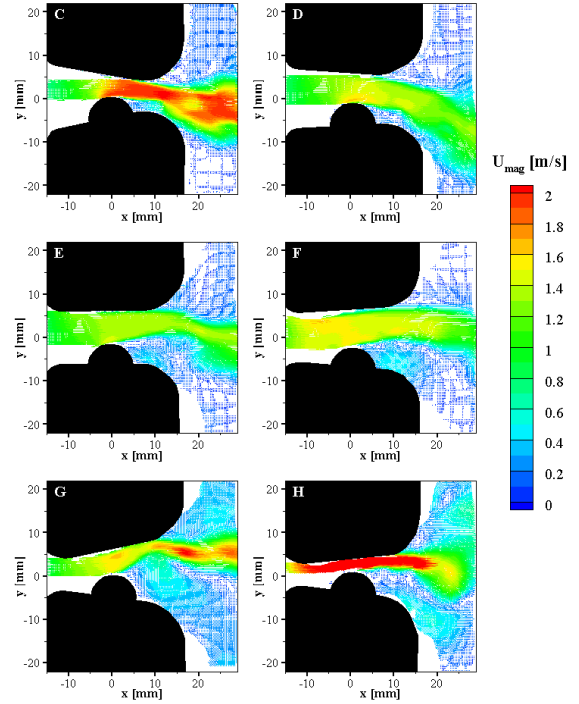


Figure 6: Mean velocity fields in the x - y plane at $z = 0$ cm.

of the polyp. As the cycle progresses and the convergent angle decreases (point D) a region of stagnant flow is observed at the location of the polyp. This corresponds with the velocity fields seen in Figure 6C, where the flow is still attached to the diseased wall, but there is a small recirculation zone. This stagnant region continues to grow, and as the vocal folds reach a divergent configuration (Figure 6F) a counter-rotating vortex pair emerges in the wake of the polyp, moving up and away from the wall. As expected, this behavior is consistent with the shedding of hairpin vortices from a sphere, where the vortex pair forms the legs of the hairpin vortex. What is unexpected is there is no observation of a horseshoe, or standing, vortex that would be expected to appear around the base of the polyp, and have an opposite rotation sense as the hairpin vortex (Acarlar and Smith, 1987). As the cycle progresses, the hairpin vortex broadens and then weakens as the vocal fold walls close. In Figure 8H there is also a significant downwash of flow towards the diseased wall. It is interesting to note that as the vocal folds close, Figure 8J, the flow in the z direction is directed away from the polyp. However, at the start of the cycle, Figure 8A, the flow in the z direction is directed towards the polyp. It must be remembered, however, that there is a significant duration of time between the acquisition times of Figure 8J, and Figure 8A (see Figure 3). This change in flow orientation from Figure 8J to 8A may arise due to effects caused by the displacement of the flow due to wall motion as the glottis opens.

In Figure 9, the out-of-plane velocity fields are computed at $x = 1.5$ cm. Behavior is similar to that shown in Figure 8, with flow directed towards the polyp during the opening

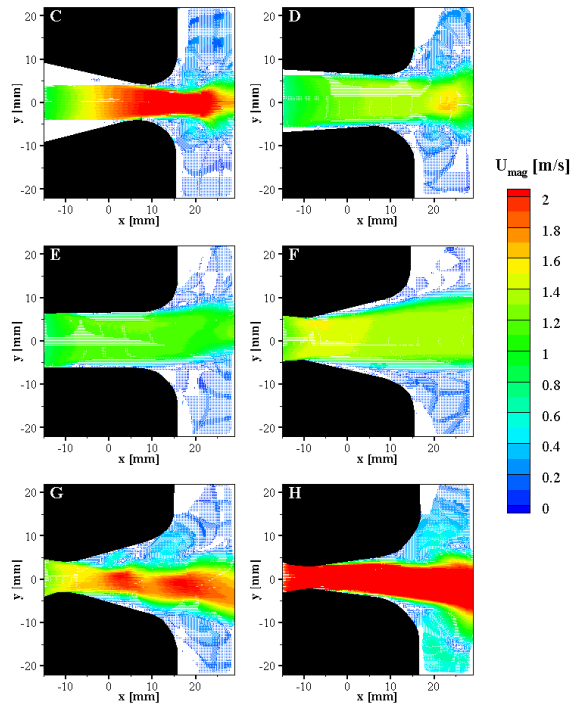


Figure 7: Mean velocity fields in the x - y plane at $z = 1.0$ cm.

phases, and the emergence of a hairpin vortex as the vocal fold walls form a divergent passage. Similarly, in Figure 9J, there is also a significant increase in the magnitude of the flow that is directed towards the damaged wall. However, upon closer inspection, directly along the diseased wall, the flow is moving away from the wall, in direct opposition to the dominant flow velocity. As the cycle progresses to point J, this flow away from the wall forms into the emergence of a horseshoe vortex as the motion is now down, and into the wall, rather than up, and away from it. Similar, albeit diminished, behavior can also be seen at point J, at which point the hairpin vortex has completely disappeared.

DISCUSSION AND CONCLUSIONS

The presence of a unilateral polyp gives rise to the development of hairpin vortices shedding from the protuberance. However, standing horseshoe vortices were only observed in the data plane 1.5 cm downstream of the polyp midline, and only during the closing phases of the cycle. This is surprising, as Acarlar and Smith (1987) found that the circulation of the standing vortex is $1/3$ that of the head of the hairpin vortex (that is observed in the x - y plane of Figure 6), while the circulation in the legs of the hairpin vortex were found to be $1/7$ of that in the head. Therefore, it is expected that the horseshoe vortex would dominate the flow pattern, when in fact, the opposite occurs. However, it should be remembered that the current investigations were not in steady flow, and had the added complexity of moving walls, and an opposing boundary that is on order with the height of the

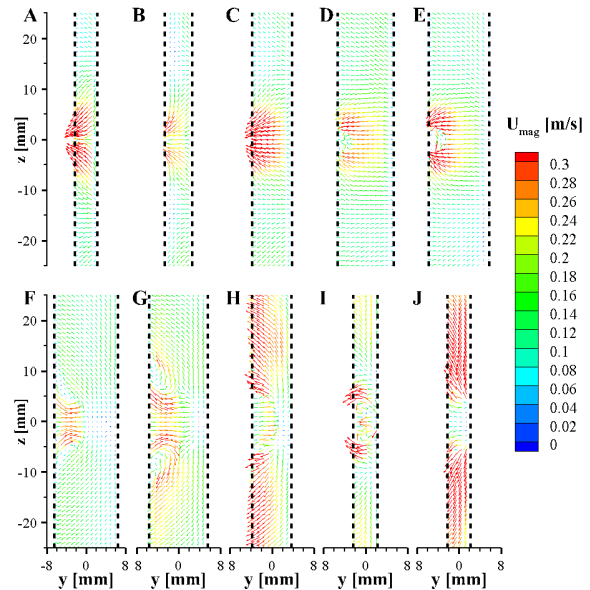


Figure 8: Mean velocity fields in the y - z plane at $x = 0.7$ cm.

protuberance. In particular, as the vocal folds close, and the wall pinches off the formation of the hairpin vortices, a horseshoe vortex is observed downstream of the polyp.

The implications of the observed flow patterns on the energy exchange process of speech are significant. As previously discussed, chaotic vocal fold motion in clinical investigations of speech where a polyp is present have neglected the role of complex flow patterns as an explanation for the observance of chaotic vocal fold dynamics. However, these investigations have shown that when a unilateral polyp is present, the flow field is significantly altered, with the emergence of significant three-dimensional flow effects. The appearance of hairpin vortices coincides perfectly with the glottal jet shifting from the diseased to the opposing wall in the x - y plane (Figure 6). This most likely occurs due to the induced flow of the counter-rotating vortices that is directed up and away from the diseased wall. While not explicitly observed during the opening phases of the cycle, the presence of a standing vortex around the base of the polyp, which would direct flow towards the diseased wall, may help explain why the jet in the x - y plane shown in Figure 6 consistently attaches to the diseased wall during the opening phases. As the vocal folds close, the opposing wall pinches off the formation of hairpin vortices,

Erath et al., (2011) have shown that simple flow asymmetries in pathological speech can greatly impact vocal fold dynamics. The complex flow patterns that were observed in these investigations suggest that the spatially and temporally-varying flow separation points, combined with the emergence of anterior-posterior flow asymmetries, will give rise to pressure forces that are significantly different from the relatively uniform pressure distributions that occur in normal speech. Disruptions of this magnitude are expected to greatly alter the energy-exchange process that drives vocal fold

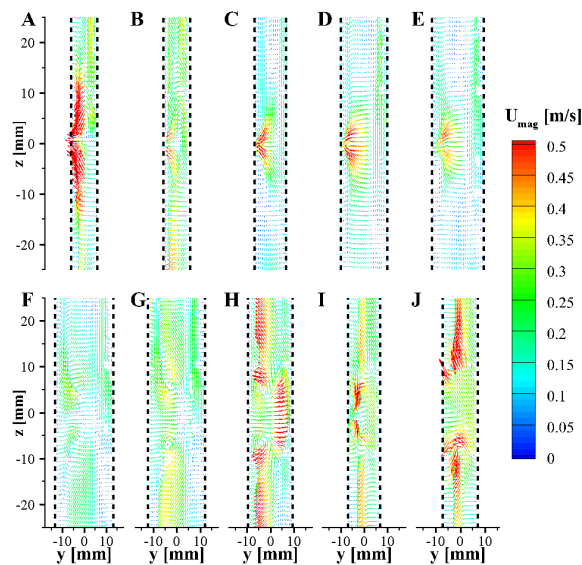


Figure 9: Mean velocity fields in the y - z plane at $x = 1.5$ cm.

motion, and should be considered as a mechanism for inciting chaotic vocal fold motion when a nodule or polyp is present.

ACKNOWLEDGEMENTS

This research was supported by Grant #CBET-0828903, 1036280 from the CBET, National Science Foundation.

REFERENCES

Acarlar, M. S., and Smith, R. S., 1987. "A Study of Hairpin Vortices in a Laminar Boundary Layer. Part 1. Hairpin Vortices Generated by a Hemisphere Protuberance," *Journal of Fluid Mechanics*, Vol. 175, pp. 1-41.

Baken, R. J., 1999. "Irregularity of Vocal Period and Amplitude: A First Approach to the Fractal Analysis of Voice," *Journal of Voice*, Vol.4, pp. 185-197.

Berry, D. A., Herzel, H., Titze, I. R., and Kirscher, K., 1994. Interpretation of Biomechanical Simulations of Normal and Chaotic Vocal Fold Oscillations with Empirical Eigenfunctions," *Journal of the Acoustical Society of America*, Vol. 95, pp. 3595-3604.

Erath, B. D., and Plesniak, M. W., 2006a, "An Investigation of Bimodal Jet Trajectory in Flow Through Scaled Models of the Human Vocal Tract," *Experiments in Fluids*, Vol. 40, pp. 683-696.

Erath, B. D., and Plesniak, M. W., 2006b, "The Occurrence of the Coanda Effect in Pulsatile Flow Through Static Models of the Human Vocal Folds," *Journal of the Acoustical Society of America*, Vol. 120: 1000-1011.

Erath, B. D., and Plesniak, M. W., 2010a. "An Investigation of Asymmetric Flow Features in a Scaled-Up Driven Model of the Human Vocal Folds," *Experiments in Fluids*, Vol. 49, pp. 131-146.

Erath, B. D., and Plesniak, M. W., 2010b. "Viscous Flow Features in Scaled-Up Physical Models of Normal and Pathological Vocal Phonation," *International Journal of Heat & Fluid Flow*, Vol. 31, pp. 468-481.

Erath, B. D., Peterson, S. D., Zaňartu, M., Wodicka, G. R., and Plesniak, M. W., 2011. "A Theoretical Model of the Pressure Field Arising from Asymmetric Intraglottal Flows Applies to a Two-Mass Model of the Vocal Folds," *Journal of the Acoustical Society of America*, in press.

Krane, M. H., Barry, M., and Wei, T., 2007. "Unsteady Behavior of Flow in a Scaled-Up Vocal Folds Model," *Journal of the Acoustical Society of America*, Vol. 122, pp. 3659-3670.

Morel, T., 1977, "Design of Two-Dimensional Wind Tunnel Contractions," *Journal of Fluids Engineering*, Vol. 99, pp. 371-378.

Roy, N., Merrill, R. N., Thibeault, S. Gray, S. D., and Smith, E. M., 2004. "Voice Disorders in Teachers and the General Population: Effects on Work Performance, Attendance, and Future Career Choices," *Journal of Speech, Language, and Hearing Research*, Vol. 47, pp. 542-551.

Scherer, R. C., Shinwari, D., DeWitt, K. J., Zhang, C., Kucinshi, B. R., and Afjeh, A. A., 2001. "Intraglottal Pressure Profiles for a Symmetric and Oblique Glottis with a Divergence Angle of 10 Degrees," *Journal of the Acoustical Society of America*, Vol. 109, pp. 1616-1630.

Titze, I. R., 1994. *Principles of Human Voice Production*, Prentice Hall.

Triep, M., Brucker, Ch., Schroder, W., 2005, "High-Speed PIV Measurements of the Flow Downstream of a Dynamic Mechanical Model of the Human Vocal Folds," *Experiments in Fluids*, Vol. 39, pp. 232-245.

Zhang, Y., and Jiang, J. J., 2004. "Chaotic Vibrations of a Vocal Fold Model with a Unilateral Polyp," *Journal of the Acoustical Society of America*, Vol. 115, pp. 1266-1269.

Zhang, Y., and Jiang, J. J., 2008. "Asymmetric Spatiotemporal Chaos Induced by a Polypoid Mass in the Excised Canine Larynx," *Chaos*, Vol. 18:043102.